Original Article

Performance of artificial intelligence in detecting the chronic total occlusive lesions of coronary artery based on coronary computed tomographic angiography

Yanying Yang[1,2#], Zhen Zhou[1#], Nan Zhang[1], Rui Wang[1], Yifeng Gao[1], Xiaowei Ran[3], Zhonghua Sun[4,5]^, Heye Zhang[6], Guang Yang[7,8,9,10], Xiantao Song[11], Lei Xu[1]

[1]Department of Radiology, Beijing Anzhen Hospital, Capital Medical University, Beijing, China; [2]Department of Radiology, Beijing Geriatric Hospital, Beijing, China; [3]Shukun (Beijing) Technology Co., Ltd., Beijing, China; [4]Discipline of Medical Radiation Science, Curtin Medical School, Curtin University, Perth, Australia; [5]Curtin Health Innovation Research Institute (CHIRI), Curtin University, Perth, Australia; [6]School of Biomedical Engineering, Sun Yat-sen University, Guangzhou, China; [7]Bioengineering Department and Imperial-X, Imperial College London, London, UK; [8]National Heart and Lung Institute, Imperial College London, London, UK; [9]Cardiovascular Research Centre, Royal Brompton Hospital, London, UK; [10]School of Biomedical Engineering & Imaging Sciences, King's College London, London, UK; [11]Department of Cardiology, Beijing Anzhen Hospital, Capital Medical University, Beijing, China

Contributions: (I) Conception and design: Y Yang, Z Zhou, X Song, L Xu; (II) Administrative support: L Xu, X Song; (III) Provision of study materials or patients: Y Yang, Z Zhou, N Zhang, R Wang, Y Gao, X Ran; (IV) Collection and assembly of data: Y Yang, Z Zhou, N Zhang; (V) Data analysis and interpretation: Y Yang, Z Zhou, Z Sun, H Zhang, G Yang; (VI) Manuscript writing: All authors; (VII) Final approval of manuscript: All authors.

[#]These authors contributed equally to this work as co-first authors.

Correspondence to: Prof. Lei Xu, MD. Department of Radiology, Beijing Anzhen Hospital, Capital Medical University, No. 2 Anzhen Rd., Chaoyang District, Beijing 100029, China. Email: leixu2001@hotmail.com; Prof. Xiantao Song, MD. Department of Cardiology, Beijing Anzhen Hospital, Capital Medical University, No. 2 Anzhen Rd., Chaoyang District, Beijing 100029, China. Email: song0929@mail.ccmu.edu.cn.

Background: Coronary chronic total occlusion (CTO) increases the risk of developing major adverse cardiovascular events (MACE) and cardiogenic shock. Coronary computed tomography angiography (CCTA) is a safe, noninvasive method to diagnose CTO lesions. With the development of artificial intelligence (AI), AI has been broadly applied in cardiovascular images, but AI-based detection of CTO lesions from CCTA images is difficult. We aim to evaluate the performance of AI in detecting the CTO lesions of coronary arteries based on CCTA images.

Methods: We retrospectively and consecutively enrolled patients with 50% stenosis, 50–99% stenosis, and CTO lesions who received CCTA scans between June 2021 and June 2022 in Beijing Anzhen Hospital. Four-fifths of them were randomly assigned to the training dataset, while the rest (1/5) were randomly assigned to the testing dataset. Performance of the AI-assisted CCTA (CCTA-AI) in detecting the CTO lesions was evaluated through sensitivity, specificity, positive predictive value, negative predictive value, accuracy, and receiver operating characteristic analysis. With invasive coronary angiography as the reference, the diagnostic performance of AI method and manual method was compared.

Results: A total of 537 patients with 1,569 stenotic lesions (including 672 lesions with <50% stenosis, 493 lesions with 50–99% stenosis, and 404 CTO lesions) were enrolled in our study. CCTA-AI saved 75% of the time in post-processing and interpreting the CCTA images when compared to the manual method (116±15 *vs.* 472±45 seconds). In the testing dataset, the accuracy of CCTA-AI in detecting CTO lesions was 86.2% (79.0%, 90.3%), with the area under the curve of 0.874. No significant difference was found in detecting CTO lesions between AI and manual methods (P=0.53).

Conclusions: AI can automatically detect CTO lesions based on CCTA images, with high diagnostic accuracy and efficiency.

^ ORCID: 0000-0002-7538-4761.

Keywords: Chronic total occlusion (CTO); coronary computed tomography angiography (CCTA); artificial intelligence (AI); diagnostic performance

Submitted Oct 21, 2023. Accepted for publication Apr 19, 2024. Published online Jun 20, 2024.
doi: 10.21037/cdt-23-407
View this article at: https://dx.doi.org/10.21037/cdt-23-407

Introduction

Background

Coronary chronic total occlusion (CTO) refers to a total occlusion of a coronary artery over a period of 3 months, as evidenced by angiography or clinical examination (1). Around patients with coronary artery disease 30% of them will develop CTO, which increases the risk of developing major adverse cardiovascular events (MACE) and cardiogenic shock (2,3). To achieve success with percutaneous coronary intervention (PCI) for CTO lesions, a high level of technical skill is required as well as extensive planning (1). Performing a pre-procedure assessment of both the lesion characteristics and the anatomy of the CTO is critical to improving the procedure's success and the prognosis of the patient (4).

Highlight box

Key findings

- Artificial intelligence (AI) can automatically identify coronary chronic total occlusion (CTO) lesions with high diagnostic accuracy and efficiency.

What is known and what is new?

- The pre-procedure assessment of the CTO is critical to improving the procedure's success and the prognosis of the patients. The manual procedure of detecting CTO lesions using coronary computed tomography angiography (CCTA) is time-consuming and laborious. AI has been applied in detecting cardiovascular diseases, but in the detection of CTO lesions is difficult, and few studies have assessed its performance.
- We proposed a new AI algorithm to detect CTO lesions, which is with good diagnostic accuracy and efficiency.

What is the implication, and what should change now?

- AI is an automatic vascular segmentation and analysis tool with promising possibilities and applications. With the progress of the continuous evolution of algorithms, the accuracy and the clinical implementation will be further increased.

Rationale and knowledge gap

Coronary computed tomography angiography (CCTA) is a safe, noninvasive method to diagnose CTO lesions (5,6). It enables visualization of fine morphological features and anatomical details of CTO lesions, including proximal stump morphology, the length of lesion, the extent of calcification, and the tortuosity of vessel (7) which are important for grading CTO before PCI (8). A preprocedural CCTA guided-CTO procedure resulted in a higher success rate with numerically fewer immediate periprocedural complications (6).

However, the manual procedure of detecting and evaluating CTO lesions using CCTA not only requires complicated three-dimensional post-processing, which is time-consuming and laborious but also highly relies on the experience of radiologists, which is prone to subjective variability errors. It is therefore important to develop a method for detecting and assessing CTO lesions that is more efficient and objective.

With the development of artificial intelligence (AI), great changes have occurred in cardiovascular imaging. Owing to its superior performance in medical image analysis, AI has been broadly applied in cardiovascular image quality optimization (9), structure segmentation (10,11), lesion feature extraction (12), risk stratification (13), aided diagnosis (14,15), guidance of treatment decision (16) and prognosis assessment (17). Moreover, AI has also been used to automatically assess collateral physiology in CTO using angiography and automatically segment and reconstruct for CT of CTO (18,19).

However, the reduction in the contrast medium at the occlusion site or the distal vessel is prone to cause vessel segmentation errors, following which, the vessel segments were disconnected, and those before and after occlusion were difficult to be demonstrated in reconstructed images. AI-based detection of CTO lesions from CCTA images is difficult, and few studies have assessed its performance in

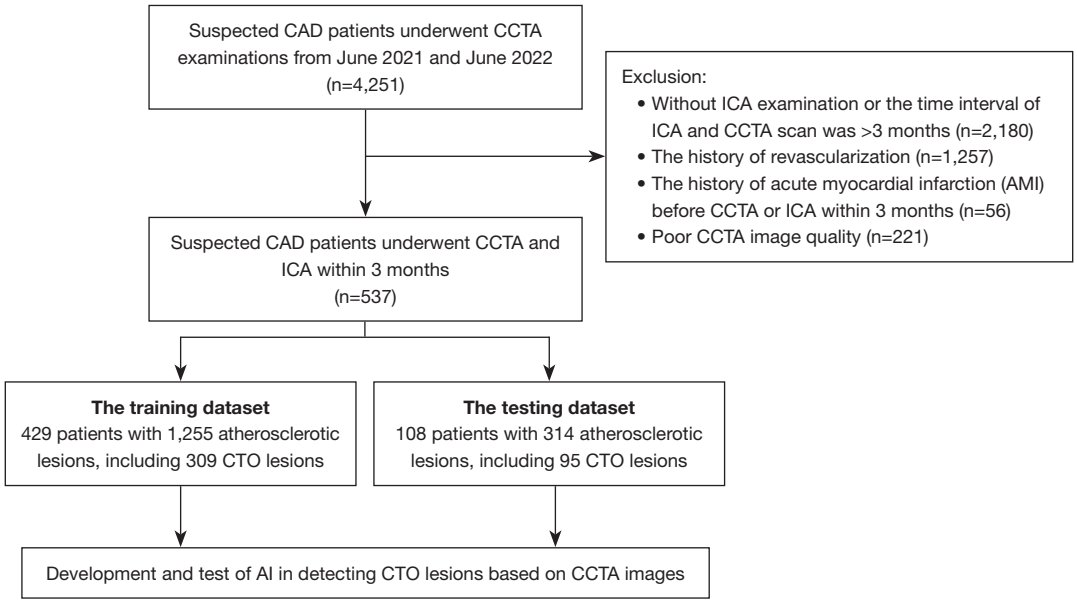

Figure 1 Flowchart of the study population enrollment. CAD, coronary atherosclerosis disease; CCTA, coronary computed tomography angiography; ICA, invasive coronary angiography; CTO, chronic total occlusion; AI, artificial intelligence.

this area.

Objective

In this study, we aimed to develop a new AI model to automatically detect CTO lesions based on CCTA images, compared with the manual diagnosis of CTO lesions, with invasive coronary angiography (ICA) as the reference standard. We present this article in accordance with the STARD reporting checklist (available at https://cdt.amegroups.com/article/view/10.21037/cdt-23-407/rc).

Methods

Study population

To reduce patient selection bias, we retrospectively and consecutively reviewed patients with suspected coronary atherosclerosis disease (CAD) who underwent CCTA examinations from June 2021 and June 2022 in Beijing Anzhen Hospital. The patients were finally included according to the inclusion and exclusion criteria of our study. They were randomly assigned to the training dataset and the testing dataset at a rate of 4:1 (*Figure 1*). The explanation of allocation of the training set and the test set, and determination of the sample size was shown in Appendix 1.

The exclusion criteria are as follows: (I) without ICA examination or more than 3 months between ICA and CCTA; (II) history of revascularization; (III) history of acute myocardial infarction (AMI) before CCTA or ICA within 3 months; (IV) poor CCTA image quality.

The study was conducted in accordance with the Declaration of Helsinki (as revised in 2013). The study was approved by the institutional ethics board of Beijing Anzhen Hospital in China (No. 2021164X) and informed consent was obtained from all the patients.

CCTA scanning protocols and analysis

All patients were scanned using a dual-source computed tomography (CT) scanner (Somatom Definition Flash, Siemens Healthineers, Forchheim, Germany) and a 256-slice CT scanner (Revolution CT, GE Healthcare, Milwaukee, WI, USA) within 3 months before ICA. We used retrospectively echocardiographic gating for all scans. The acquisition was triggered by a bolus tracking technique and the region of interest was placed in the ascending aorta. During CT scan, 0.8 mL/kg of contrast (Iohexol 350, GE Ltd., Boston, MA, USA) was injected at a flow rate of 4.0–5.0 mL/s followed by a 30 mL saline flush. Details of the scan parameters are as follows: (I) dual-source CT scanner: rotation time 0.28 seconds, pixel matrix 512×512,

collimation 2×64×0.6 mm, tube voltage 100 or 120 kV, with automatically selected tube current. The slice thickness was 0.6 mm with a reconstruction increment of 0.4 mm; (II) 256-slice CT scanner: rotation time 0.28 seconds, pixel matrix 512×512, collimation 256×0.625 mm, tube voltage 100 or 120 kV, and the Smart mA was applied. The slice thickness was 0.625 mm with a reconstruction increment of 0.4 mm. Radiation dose estimates for CCTA were calculated using recommended conversion factors, k =0.014 $mSvd \cdot mGy^{-1} \cdot cm^{-1}$ (20).

Two experienced radiologists (both with >5-year experience in cardiovascular image analysis) analyzed the CCTA images using a commercial workstation (Vitrea fx3.0, Canon Corporation, Tokyo, Japan). They independently reconstructed and detected the lesions with ≥50% stenosis (including CTO lesions) and were blinded to the results of the ICA. Quantitative assessment of coronary stenosis was performed according to the Society of Cardiovascular Computed Tomography (SCCT) guidance (21). This study included coronary arteries with diameter of 1.5 mm or more. The coronary lesions with ≥50% stenosis (including CTO lesions) was considered positive (22,23). Image analysis time was recorded from loading the images to the diagnosis of all target lesions.

Deep learning (DL) model for coronary CTO lesions segmentation and detection

To achieve myocardial and coronary artery segmentation and target lesion identification, convolutional neural network (CNN) was used, which include feed-forward neuronal networks and contain neurons with learnable weights and biases (24). The proposed DL framework consisted of three models: (I) a two-stage 3D U-Net-based myocardium segmentation network to determine the coordinates of the heart contour and segment the myocardium fine structure; (II) a modified 3D U-Net for coronary segmentation, which includes encoding and decoding parts, and a connected growth prediction model (CGPM) to eliminate vascular segmentation errors and then avoid partial or missing vascular segments of CTO lesions effectively; and (III) a vessel-connect algorithm to identify the missing segments of the vessels and connect them with main branches, which in turn localizes and displays the region of CTO lesions (*Figure 2*). Detailed steps regarding our AI model development are shown in Appendix 2.

Statistical analysis

Statistical analysis was performed using SPSS version 23 (SPSS, Chicago, IL, USA). Continuous variables are presented as mean ± standard deviation if they are normally distributed, or as median and IQR if they are not. Using the probability-probability plot, a normal distribution was assessed. Categorical variables are expressed as the number and percentage. Using independent *t*-tests and Mann-Whitney *U* tests, we compared differences in continuous and dichotomous demographic information between the training dataset and the testing dataset. Diagnostic performance of the AI was evaluated through sensitivity, specificity, positive predictive value (PPV), negative predictive value (NPV), and accuracy. McNemar's test and receiver operating characteristic (ROC) analysis was also used to evaluate the accuracy of AI method and manual method with ICA as the reference in detecting coronary CTO lesions and lesions with 50–99% stenosis. The area under the curve (AUC) =0.50 was considered a valueless diagnostic indicator, 0.50< AUC ≤0.7 was low diagnostic accuracy, 0.7< AUC ≤0.9 was moderate, and 0.9< AUC ≤1.0 was good. Intra-class correlation coefficient (ICC) test was used to evaluate the intra-observer and inter-observer consistency, using a two-way random model and the absolute agreement definition. ICC value ≥0.75 indicates good reliability; 0.4≤ ICC <0.75 indicates medium reliability; <0.40 indicates poor reliability. Two-tailed P<0.05 was considered to have a significant difference.

Results

The demographics of the patients

Detailed demographics for the training and the testing dataset are shown in *Table 1*. A total of 537 patients with 1,569 ICA-confirmed atherosclerotic lesions (including 672 lesions with <50% stenosis, 493 lesions with 50–99% stenosis, and 404 CTO lesions) were finally included. In the training dataset, there were 429 patients with 1,255 atherosclerotic lesions (including 550 lesions with <50% stenosis, 396 lesions with 50–99% stenosis, and 309 CTO lesions). In the testing dataset, there were 108 patients with 314 atherosclerotic lesions (including 122 lesions with <50% stenosis, 97 lesions with 50–99% stenosis, and 95 CTO lesions). There was no notable difference in the demographic characteristics of the patients included in the

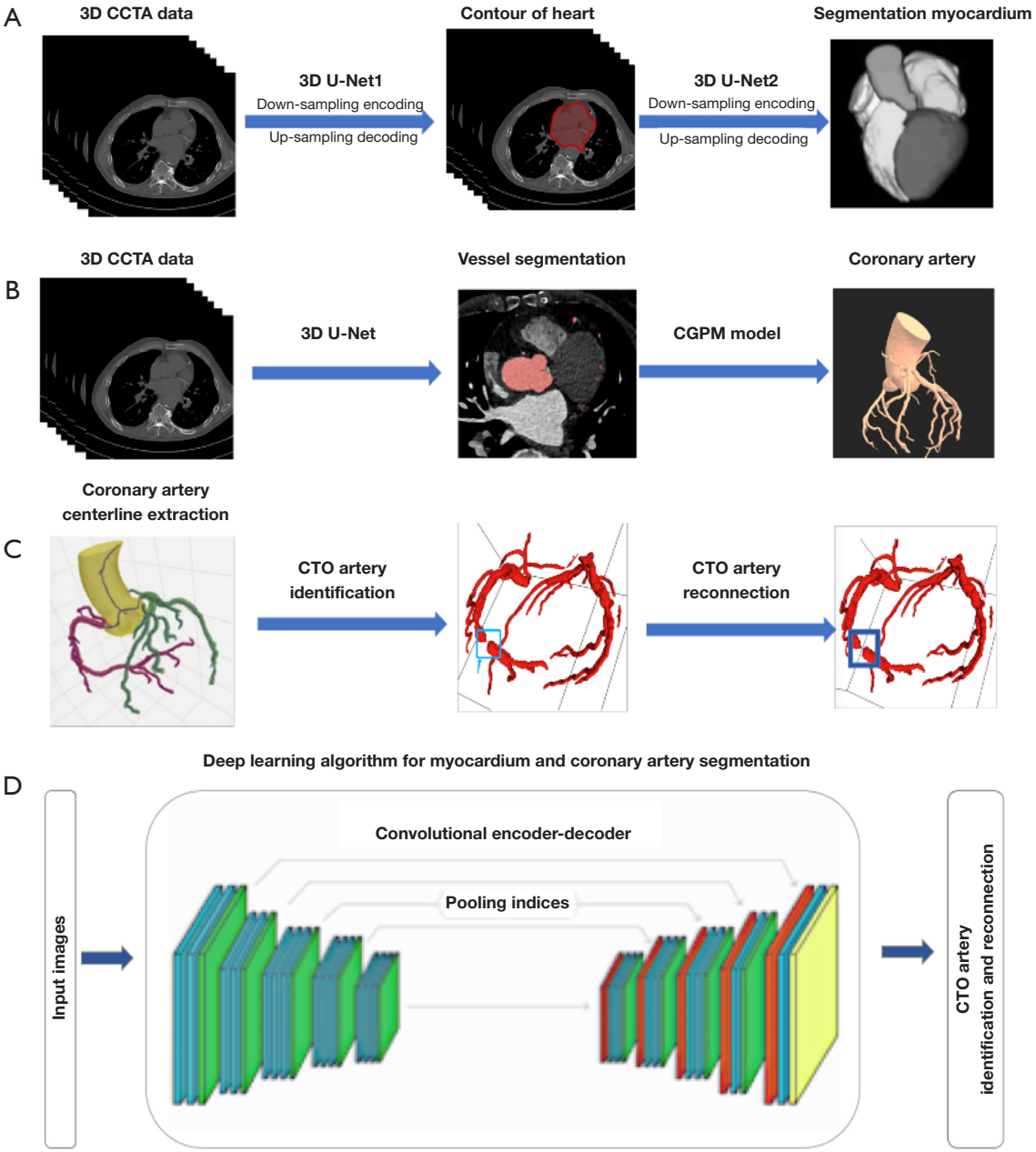

Figure 2 Overview of the proposed AI algorithm in detecting CTO lesions. The proposed deep learning framework consisted of three models: (A) a two-stage 3D U-net-based myocardium segmentation network (red contour: contour of heart); (B) a modified 3D U-Net for coronary segmentation; (C) a vessel-connect algorithm to identify the missing segments of the vessels and connect them with main branches (blue boxes: CTO lesions). (D) Flowchart of the proposed AI algorithm in detecting CTO lesions. CCTA, coronary computed tomography angiography; CGPM, connected growth prediction model; CTO, chronic total occlusion; AI, artificial intelligence.

Table 1 Patient's demographics characteristics

Characteristics	Training dataset (N=429)	Testing dataset (N=108)	P value
Male	351 (81.8)	93 (86.1)	0.29
Age (years)	59.9±9.7	59.4±10.9	0.16
BMI (kg/m^2)	26.1±3.6	26.0±3.5	0.59
Coronary risk factors			
Hypertension	273 (63.6)	61 (56.5)	0.17
Hyperlipidemia	272 (63.4)	68 (63.0)	0.90
Diabetes mellitus	143 (33.3)	37 (34.3)	0.86
Smoking	227 (52.9)	58 (53.7)	0.90
Drinking	75 (17.5)	24 (22.2)	0.26

Values are mean ± standard deviation or n (%). BMI, body mass index.

training and testing datasets. The mean effective radiation dose of the CT exam was 3.2±2.2 mSv.

Efficiency of AI in locating and detecting coronary CTO lesions and lesions with 50–99% stenosis

Compared to the traditional manual post-processing and diagnostic method (CCTA-manual, 472±45 seconds), the average time of our AI-assisted post-processing method in CCTA (CCTA-AI) for each patient was dramatically reduced to 116±15 seconds and reduced time by 75%, and the report was also automatically generated.

Accuracy of AI in locating and detecting coronary CTO lesions and lesions with 50–99% stenosis

Table 2 shows the diagnostic performance of CCTA-AI and CCTA-manual in identifying CTO lesions and lesions with 50–99% stenosis. The example of the lesion detection of the CCTA-AI method was shown in *Figure 3*.

With ICA as the reference method in locating and detecting CTO lesions, the sensitivity, specificity, PPV, NPV, and accuracy of CCTA-AI in the training dataset were 90.3% (86.3%, 93.3%), 98.1% (95.1%, 99.2%), 98.2% (95.2%, 99.4%), 89.2% (84.8%, 92.5%), 93.8% (91.4%, 95.5%), and 80.0% (70.3%, 87.2%), 96.4% (86.8%, 99.3%), 97.4% (90.2%, 99.5%), 74.3% (62.6%, 83.5%), 86.2% (79.0%, 90.3%) in the testing dataset. No significant difference was found in detecting CTO lesions between AI and manual method (P=0.12 and 0.53). The ROC analysis showed good and moderate accuracy of CCTA-AI in the training dataset and the testing dataset (AUC =0.942 and 0.874) (*Figure 4*).

In locating and detecting lesions with 50–99% stenosis, the sensitivity, specificity, PPV, NPV, and accuracy of CCTA-AI in the training dataset were 92.7% (88.7%, 95.5%), 97.7% (95.2%, 99.0%), 97.1% (93.8%, 98.7%), 94.7% (91.1%, 96.6%), 95.5% (93.5%, 97.0%), and 87.7% (75.7%, 94.5%), 97.9% (91.9%, 99.6%), 96.1% (85.7%, 99.3%), 93.0% (85.6, 96.9%), 94.1% (89.0%, 97.0%) in the testing dataset. No significant difference was found in detecting lesions with 50–99% stenosis between AI and manual methods (P=0.82 and 0.75). The ROC analysis also showed good accuracy of CCTA-AI in the training dataset and the testing dataset (AUC =0.953 and 0.928) (*Figure 4*). However, the proposed AI method in differentiating the ICA confirmed subtotal occlusion (STO) (95%≤ stenosis <100%), which is a "functional" total occlusion or a slow contrast penetration through the occluded segment, and CTO lesions (100%) was found to be poor, with the sensitivity, specificity, PPV, NPV and accuracy of CCTA-AI in the training dataset (STO n=117) was 53.0% (43.6%, 62.2%), 79.6% (74.6%, 83.9%), 49.6% (40.6%, 58.6%), 81.7% (76.8%, 85.8%), 72.3% (67.0%, 75.9%), and 45.2% (27.8%, 63.7%), 75.8% (65.7%, 83.7%), 37.8% (22.9%, 55.2%), 80.9% (70.9%, 88.2%), 68.3% (61.8%, 78.2%) in the testing dataset (STO n=31) (*Table 3*).

Both intra-observer and inter-observer agreements were good (ICC =0.933 for observer A, ICC =0.905 for observer B, and ICC =0.891 for inter-observer agreement, all P<0.05).

Table 2 Diagnostic performance of CCTA-AI and CCTA-manual in detecting CTO lesions and lesions with 50–99% stenosis

Variables	Training dataset				Testing dataset			
	CTO lesions		Lesions with 50–99% stenosis		CTO lesions		Lesions with 50–99% stenosis	
	CCTA-AI	CCTA-manual	CCTA-AI	CCTA-manual	CCTA-AI	CCTA-manual	CCTA-AI	CCTA-manual
Number of lesions	309	309	396	396	95	95	97	97
Sensitivity (95% CI) (%)	90.3 (86.3, 93.3)	86.7 (82.3, 90.2)	92.7 (88.7, 95.5)	92.4 (88.2, 95.2)	80.0 (70.3, 87.2)	83.2 (73.8, 89.9)	87.7 (75.7, 94.5)	91.2 (80.0, 96.7)
Specificity (95% CI) (%)	98.1 (95.1, 99.2)	97.6 (94.6, 99.0)	97.7 (95.2, 99.0)	98.0 (95.6, 99.2)	96.4 (86.8, 99.3)	96.5 (86.8, 99.4)	97.9 (91.9, 99.6)	96.7 (90.4, 99.2)
Positive predictive value (95% CI) (%)	98.2 (95.2, 99.4)	97.8 (95.1, 99.1)	97.1 (93.8, 98.7)	95.8 (93.3, 97.9)	97.4 (90.2, 99.5)	97.5 (90.5, 99.5)	96.1 (85.7, 99.3)	94.5 (83.9, 98.6)
Negative predictive value (95% CI) (%)	89.2 (84.8, 92.5)	85.7 (81.0, 89.4)	94.7 (91.1, 96.6)	95.3 (91.8, 97.3)	74.3 (62.6, 83.5)	67.9 (63.7, 81.2)	93.0 (85.6, 96.9)	94.8 (87.8, 98.1)
Accuracy (95% CI) (%)	93.8 (91.4, 95.5)	91.6 (89.0, 93.7)	95.5 (93.5, 97.0)	95.5 (93.4, 97.1)	86.2 (79.0, 90.3)	88.2 (82.0, 92.5)	94.1 (89.0, 97.0)	94.7 (89.8, 97.5)
P value	0.12		0.82		0.53		0.75	

CCTA, coronary computed tomography angiography; AI, artificial intelligence; CTO, chronic total occlusion; CI, confidence interval.

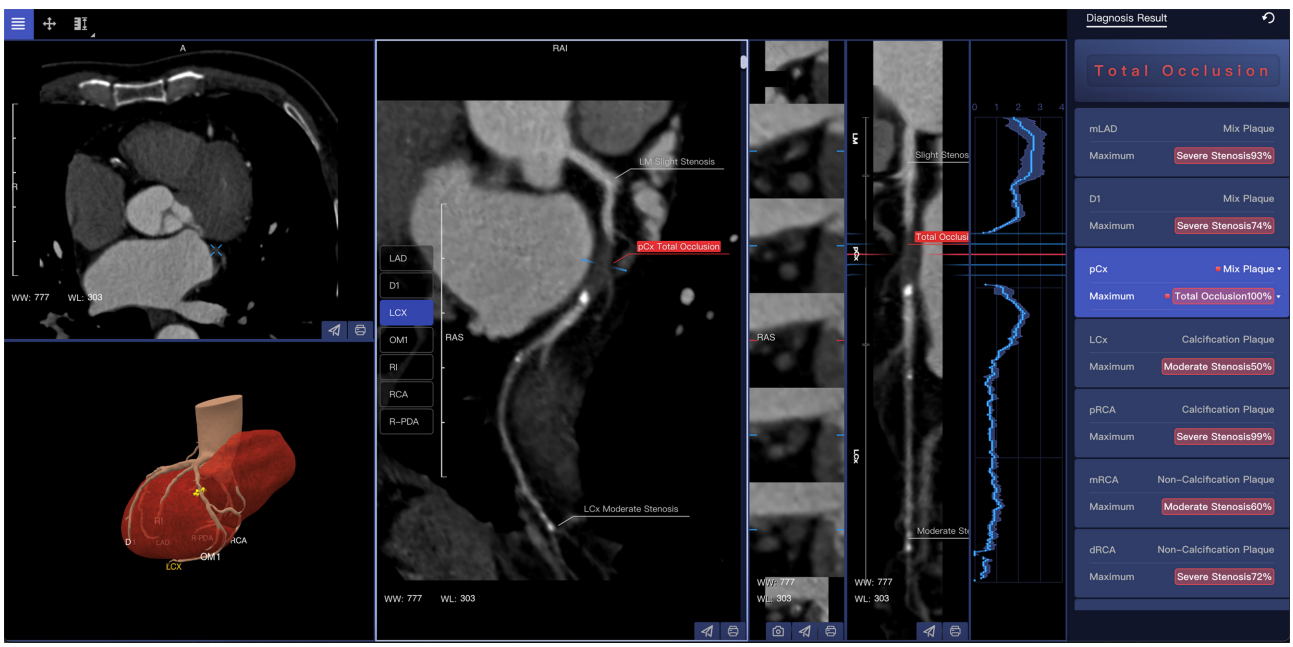

Figure 3 Example of the lesion detection of the proposed AI-assisted CCTA method. A chronic total occlusion lesion in the proximal segment of LCX was automatedly detected, and the reports are generated automatically. WW, window width; WL, window level; LAD, left anterior descending artery; D1, first diagonal branch; LCX, left circumflex artery; OM1, first obtuse margin branch; RI, ramus intermedius; RCA, right coronary artery; R-PDA, right posterior descending artery; LM, left main coronary artery; pCx, proximal segment of the LCX; mLAD, middle segment of the LAD; pRCA, proximal segment of the RCA; mRCA, middle segment of the RCA; dRCA, distal segment of the RCA; AI, artificial intelligence; CCTA, coronary computed tomography angiography.

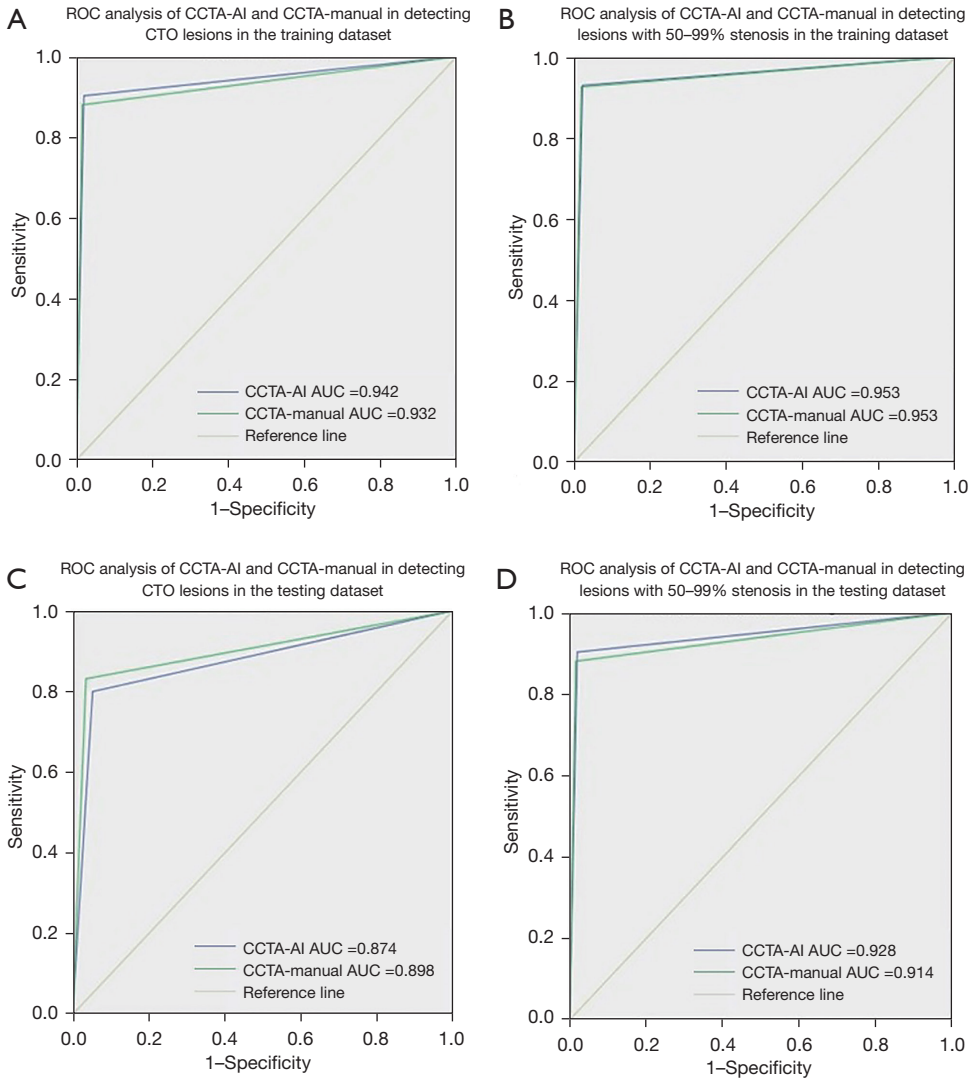

Figure 4 ROC analysis of CCTA-AI and CCTA-manual in detecting CTO lesions and lesions with 50–99% stenosis. (A) ROC analysis of CCTA-AI and CCTA-manual in detecting CTO lesions in the training dataset; (B) ROC analysis of CCTA-AI and CCTA-manual in detecting lesions with 50–99% stenosis in the training dataset; (C) ROC analysis of CCTA-AI and CCTA-manual in detecting CTO lesions in the testing dataset; (D) ROC analysis of CCTA-AI and CCTA-manual in detecting lesions with 50–99% stenosis in the testing dataset. ROC, receiver operating characteristic; CCTA, coronary computed tomography angiography; AI, artificial intelligence; CTO, chronic total occlusion; AUC, area under the curve.

Discussion

Key findings

In our study, we proposed a new AI model to facilitate automated segmentation and detection of CTO lesions, which is more efficient than traditional manual image reconstruction and diagnosis (reduces 75% of time to reconstruct and interpret images). With ICA as the reference method, the accuracy of CCTA-AI in the detection of CTO lesions and lesions with 50–99% stenosis is good, and no significant difference is revealed between the AI method and the manual method.

Comparison with similar researches and explanations of findings

DL has been shown to be a promising tool in image segmentation and recognition (25,26). AI applies CNN

Table 3 Diagnostic performance of CCTA-AI and CCTA-manual in detecting STO lesions

Variables	Training dataset		Testing dataset	
	CCTA-AI	CCTA-manual	CCTA-AI	CCTA-manual
Number of lesions	117	117	31	31
Sensitivity (95% CI) (%)	53.0 (43.6, 62.2)	64.1 (54.7, 72.6)	45.2 (27.8, 63.7)	61.3 (42.3, 77.6)
Specificity (95% CI) (%)	79.6 (74.6, 83.9)	85.8 (81.2, 89.4)	75.8 (65.7, 83.7)	84.2 (75.0, 90.6)
Positive predictive value (95% CI) (%)	49.6 (40.6, 58.6)	63.0 (53.6, 71.6)	37.8 (22.9, 55.2)	55.9 (38.1, 72.4)
Negative predictive value (95% CI) (%)	81.7 (76.8, 85.8)	86.3 (81.8, 89.9)	80.9 (70.9, 88.2)	87.0 (77.9, 92.8)
Accuracy (95% CI) (%)	72.3 (67.0, 75.9)	79.8 (71.5, 85.2)	68.3 (61.8, 78.2)	78.6 (68.3, 84.4)
P value	0.66		0.78	

CCTA, coronary computed tomography angiography; AI, artificial intelligence; STO, subtotal occlusion; CI, confidence interval.

to achieve vessel extraction, automatically identifying main vessels and branches and generating high-quality reconstructed images, which fulfilled the requirement for clinical routine diagnosis and thus has been widely used in the evaluation of CAD. To detect coronary arterial lesions with stenosis, Kang *et al.* (27) proposed a structured learning technique, with good sensitivity, specificity, and accuracy achieved. Promising results were demonstrated in the automated detection of obstructive and nonobstructive lesions from CCTA. A multi-center, international study (CLARIFY study) additionally validated the capability of AI-assisted analysis in swiftly and precisely assessing vessel shape and narrowing (14). Some studies have also confirmed that DL algorithms exhibited excellent diagnostic accuracy in coronary atherosclerotic conditions, while also considerably decreasing the duration of post-processing and interpretation of CCTA images (15,19).

However, the reduction in the contrast medium at the occlusion site or the distal vessel is prone to cause vessel segmentation errors, following which, the vessel segments were disconnected, and those before and after occlusion were difficult to be demonstrated in reconstructed images, which brings challenges in the automatic location and detection for CTO lesions. Only a few research papers on AI in the segmentation and reconstruction of CTO lesions were published (19), resulting in decreased time required for postprocessing CTO quantification and demonstrating strong correlation and agreement in the anatomical evaluation of occlusion characteristics. However, no previous reports have investigated the performance of AI in detecting CTO lesions, and additional research is necessary to develop a completely automated algorithm for the segmentation, reconstruction, and identification of CTOs.

To solve the problem of automatically detecting the CTO lesions of the coronary arteries, we developed a new DL algorithm to enable automated extraction of the centerlines of coronary arteries and locate the CTO lesions by completing the missing segments. Based on myocardial segmentation and coronary segmentation results, we labeled each branch of the centerline and identified the missing segments of the vessels, which in turn located and displayed the CTO lesions and increased the ability of CTO lesions detection. Consequently, AI was confirmed to be a simple, reliable, and efficient tool to detect CTO lesions.

With the ICA as the reference standard, we found that the proposed AI model demonstrates commendable diagnostic capabilities not only in detecting CTO lesions but also coronary arteries lesions with 50–99% stenosis. Furthermore, our proposed AI method saved 75% of time in post-processing and interpreting the CCTA images when compared to the traditional manual method. The diagnostic accuracy of the CCTA-AI method in detecting CTO lesions (86.2% in the testing dataset) and lesions with 50–99% was good (94.1% in the testing dataset). The ROC analysis showed moderate accuracy and good accuracy of CCTA-AI in CTO lesions and lesions with 50–99% stenosis (AUC =0.874 and 0.928 in the testing dataset, respectively). No significant difference was found in detecting CTO lesions between AI and manual methods (P<0.05), but in some conditions such as the presence of larger vascular branches

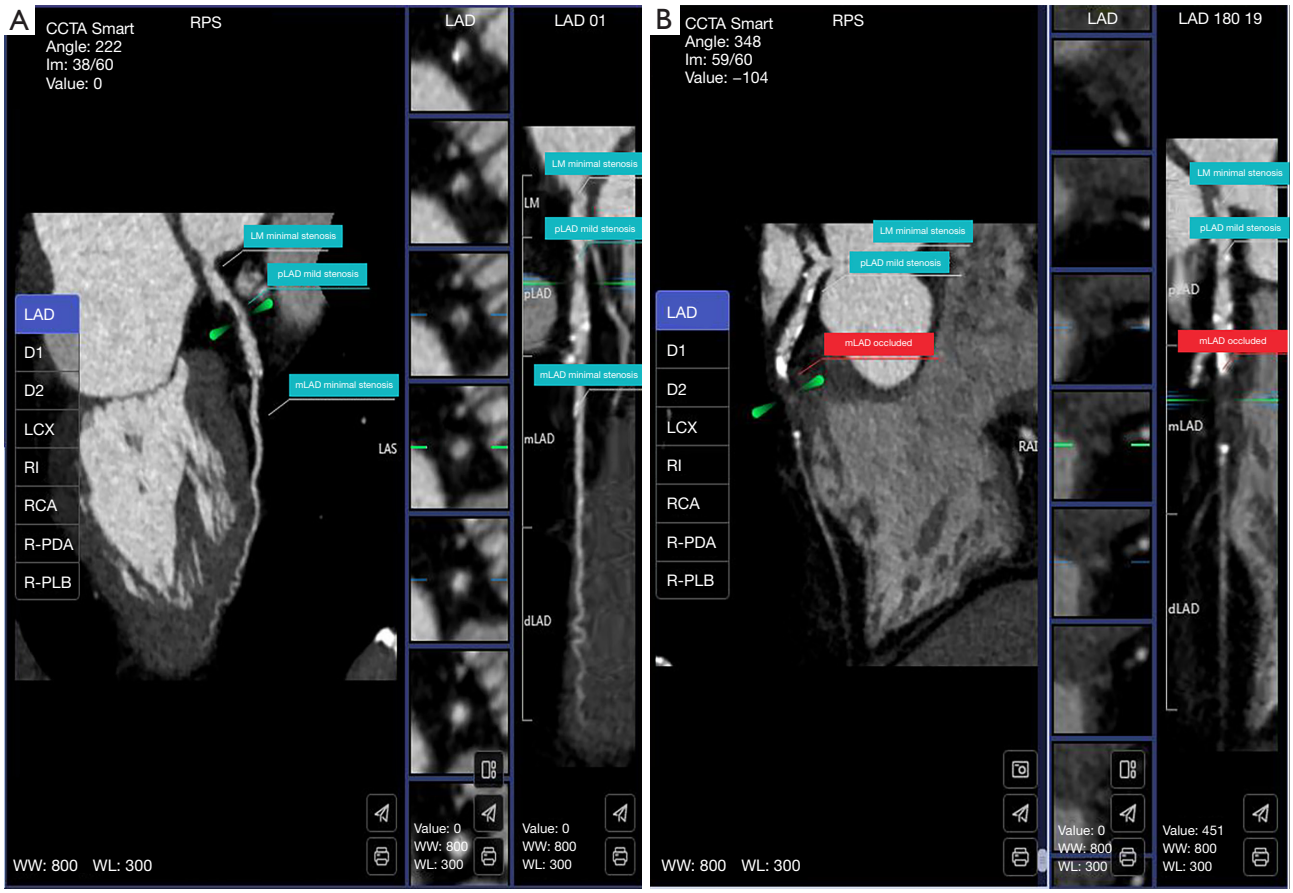

Figure 5 Example of the AI misrecognition of CTO lesion in a patient with a large vascular branch in close proximity to the occluded segment. (A) AI recognition errors occurred in LAD; (B) correct recognition of CTO lesion in LAD after manual adjustment. CCTA, coronary computed tomography angiography; LAD, left anterior descending artery; D1, first diagonal branch; D2, second diagonal branch; LCX, left circumflex artery; RI, ramus intermedius; RCA, right coronary artery; R-PDA, right posterior descending artery; R-PLB, right posterior lateral branch; WW, window width; WL, window level; LM, left main coronary artery; pLAD, proximal segment of the LAD; mLAD, middle segment of the LAD; dLAD, distal segment of the LAD; AI, artificial intelligence; CTO, chronic total occlusion.

in close proximity to the occluded segment (*Figure 5*) or heavy calcification (peripheral calcification: maximal encircling ≥180° and cross-sectional area ≥50%) may result in AI recognition errors, which needs to be cautious.

Besides, the effectiveness of the proposed AI approach in distinguishing between ICA-confirmed STO and CTO lesions was subpar, and the diagnostic accuracy was reduced to about 70.0%. In anatomical imaging tests, both CTO and STO lesions exhibit a complete interruption of the contrast-enhanced arterial lumen, while functional imaging tests indicate myocardial ischemia. There is still a challenge in noninvasively discriminating CTO from STO lesions (28). Further studies are needed to improve the ability of AI in the automatic segmentation and detection of CTO lesions.

Limitations

Despite the advantages of CCTA-AI in detecting CTO lesions, this study has some limitations. First, the sample size was small as this study was based on a single-center experience. In the following study, we will aim to enroll multicenter data to further test and improve the performance of AI in detecting CTO lesions. Second, we did not differentiate the early and late stages of CTO lesions, which might cause some misidentifications, such as a high density of non-calcified components in occlusions

of later stages compared to those in the earlier stages. The presence of microvessels in the late stage of the occlusions exhibits an increase in vascular density, making it easier to detect (29), which was a valid concern. Finally, we excluded patients with stented lesions or after coronary artery bypass grafting surgery. Furthermore, no analysis was carried out in bypass grafts as only the assessment of native vessels was included.

Conclusions

AI can automatically detect CTO lesions based on CCTA images, with good diagnostic accuracy and efficiency. AI is becoming an automatic vascular segmentation and analysis tool with promising possibilities and applications. Our algorithm necessitates additional improvement, and a greater number of external validations are imperative for its clinical implementation.

Acknowledgments

Funding: This study was supported by grants from the National Key R&D Program of China (2022YFE0209800); National Natural Science Foundation of China (U1908211, 82271986); the Capital's Funds for Health Improvement and Research Foundation of China (2020-1-1052); the ERC IMI (101005122 to G.Y.); the H2020 (952172 to G.Y.); the MRC (MC/PC/21013 to G.Y.); the Royal Society (IEC/NSFC/211235 to G.Y.); Wellcome Leap Dynamic Resilience to G.Y.; the UKRI Future Leaders Fellowship (MR/V023799/1 to G.Y.).

Footnote

Reporting Checklist: The authors have completed the STARD reporting checklist. Available at https://cdt.amegroups.com/article/view/10.21037/cdt-23-407/rc

Data Sharing Statement: Available at https://cdt.amegroups.com/article/view/10.21037/cdt-23-407/dss

Peer Review File: Available at https://cdt.amegroups.com/article/view/10.21037/cdt-23-407/prf

Conflicts of Interest: All authors have completed the ICMJE uniform disclosure form (available at https://cdt.amegroups.com/article/view/10.21037/cdt-23-407/coif). Z.S. serves as an unpaid editorial board member of *Cardiovascular Diagnosis and Therapy* from September 2023 to August 2025. X.R. report that she is an employee of Shukun (Beijing) Technology Co. Ltd., China. The other authors have no conflicts of interest to declare.

Ethical Statement: The authors are accountable for all aspects of the work in ensuring that questions related to the accuracy or integrity of any part of the work are appropriately investigated and resolved. The study was conducted in accordance with the Declaration of Helsinki (as revised in 2013). The study was approved by the institutional ethics board of Beijing Anzhen Hospital in China (No. 2021164X) and informed consent was taken from all the patients.

References

1. Koelbl CO, Nedeljkovic ZS, Jacobs AK. Coronary Chronic Total Occlusion (CTO): A Review. Rev Cardiovasc Med 2018;19:33-9.
2. Qin Q, Chen L, Ge L, et al. A comparison of long-term clinical outcomes between percutaneous coronary intervention (PCI) and medical therapy in patients with chronic total occlusion in noninfarct-related artery after PCI of acute myocardial infarction. Clin Cardiol 2022;45:136-44.
3. Kim SH, Behnes M, Mashayekhi K, et al. Prognostic Impact of Percutaneous Coronary Intervention of Chronic Total Occlusion in Acute and Periprocedural Myocardial Infarction. J Clin Med 2021;10:258.
4. Brilakis ES, Mashayekhi K, Tsuchikane E, et al. Guiding Principles for Chronic Total Occlusion Percutaneous Coronary Intervention. Circulation 2019;140:420-33.
5. Sadamatsu K, Okutsu M. Cardiac Computed Tomography for Success in Percutaneous Coronary Intervention for Chronic Total Occlusion. JACC Cardiovasc Imaging 2022;15:172.
6. Hong SJ, Kim BK, Cho I, et al. Effect of Coronary CTA

on Chronic Total Occlusion Percutaneous Coronary Intervention: A Randomized Trial. JACC Cardiovasc Imaging 2021;14:1993-2004.
7. Opolski MP. Cardiac Computed Tomography for Planning Revascularization Procedures. J Thorac Imaging 2018;33:35-54.
8. Opolski MP, Achenbach S, Schuhbäck A, et al. Coronary computed tomographic prediction rule for time-efficient guidewire crossing through chronic total occlusion: insights from the CT-RECTOR multicenter registry (Computed Tomography Registry of Chronic Total Occlusion Revascularization). JACC Cardiovasc Interv 2015;8:257-67.
9. Tatsugami F, Higaki T, Nakamura Y, et al. Deep learning-based image restoration algorithm for coronary CT angiography. Eur Radiol 2019;29:5322-9.
10. Baskaran L, Maliakal G, Al'Aref SJ, et al. Identification and Quantification of Cardiovascular Structures From CCTA: An End-to-End, Rapid, Pixel-Wise, Deep-Learning Method. JACC Cardiovasc Imaging 2020;13:1163-71.
11. Jun Guo B, He X, Lei Y, et al. Automated left ventricular myocardium segmentation using 3D deeply supervised attention U-net for coronary computed tomography angiography; CT myocardium segmentation. Med Phys 2020;47:1775-85.
12. Zhang N, Yang G, Zhang W, et al. Fully automatic framework for comprehensive coronary artery calcium scores analysis on non-contrast cardiac-gated CT scan: Total and vessel-specific quantifications. Eur J Radiol 2021;134:109420.
13. Lin A, Kolossváry M, Motwani M, et al. Artificial Intelligence in Cardiovascular Imaging for Risk Stratification in Coronary Artery Disease. Radiol Cardiothorac Imaging 2021;3:e200512.
14. Choi AD, Marques H, Kumar V, et al. CT Evaluation by Artificial Intelligence for Atherosclerosis, Stenosis and Vascular Morphology (CLARIFY): A Multi-center, international study. J Cardiovasc Comput Tomogr 2021;15:470-6.
15. Han D, Liu J, Sun Z, et al. Deep learning analysis in coronary computed tomographic angiography imaging for the assessment of patients with coronary artery stenosis. Comput Methods Programs Biomed 2020;196:105651.
16. Gohmann RF, Pawelka K, Seitz P, et al. Combined cCTA and TAVR Planning for Ruling Out Significant CAD: Added Value of ML-Based CT-FFR. JACC Cardiovasc Imaging 2022;15:476-86.
17. Han D, Kolli KK, Al'Aref SJ, et al. Machine Learning Framework to Identify Individuals at Risk of Rapid Progression of Coronary Atherosclerosis: From the PARADIGM Registry. J Am Heart Assoc 2020;9:e013958.
18. Liu L, Ding F, Shen Y, et al. Automatic assessment of collaterals physiology in chronic total occlusions by means of artificial intelligence. Cardiol J 2023;30:685-95.
19. Li M, Ling R, Yu L, et al. Deep Learning Segmentation and Reconstruction for CT of Chronic Total Coronary Occlusion. Radiology 2023;306:e221393.
20. Shrimpton PC, Hillier MC, Lewis MA, et al. National survey of doses from CT in the UK: 2003. Br J Radiol 2006;79:968-80.
21. Leipsic J, Abbara S, Achenbach S, et al. SCCT guidelines for the interpretation and reporting of coronary CT angiography: a report of the Society of Cardiovascular Computed Tomography Guidelines Committee. J Cardiovasc Comput Tomogr 2014;8:342-58.
22. Meijboom WB, Meijs MF, Schuijf JD, et al. Diagnostic accuracy of 64-slice computed tomography coronary angiography: a prospective, multicenter, multivendor study. J Am Coll Cardiol 2008;52:2135-44.
23. Arbab-Zadeh A, Miller JM, Rochitte CE, et al. Diagnostic accuracy of computed tomography coronary angiography according to pre-test probability of coronary artery disease and severity of coronary arterial calcification. The CORE-64 (Coronary Artery Evaluation Using 64-Row Multidetector Computed Tomography Angiography) International Multicenter Study. J Am Coll Cardiol 2012;59:379-87.
24. Korb E, Bağcıoğlu M, Garner-Spitzer E, et al. Machine Learning-Empowered FTIR Spectroscopy Serum Analysis Stratifies Healthy, Allergic, and SIT-Treated Mice and Humans. Biomolecules 2020;10:1058.
25. Atasever S, Azginoglu N, Terzi DS, et al. A comprehensive survey of deep learning research on medical image analysis with focus on transfer learning. Clin Imaging 2023;94:18-41.
26. Hesamian MH, Jia W, He X, et al. Deep Learning Techniques for Medical Image Segmentation: Achievements and Challenges. J Digit Imaging 2019;32:582-96.
27. Kang D, Dey D, Slomka PJ, et al. Structured learning algorithm for detection of nonobstructive and obstructive coronary plaque lesions from computed tomography angiography. J Med Imaging (Bellingham) 2015;2:014003.
28. Choi JH, Kim EK, Kim SM, et al. Noninvasive

Discrimination of Coronary Chronic Total Occlusion and Subtotal Occlusion by Coronary Computed Tomography Angiography. JACC Cardiovasc Interv 2015;8:1143-53.
29. Wu Q, Yu M, Li Y, et al. Natural History of Untreated Coronary Total Occlusions Revealed with Follow-Up Semi-Automated Quantitative Coronary CT Angiography: The Morphological Characteristics of Initial CT Predict Occlusion Shortening. Korean J Radiol 2018;19:256-64.

Cite this article as: Yang Y, Zhou Z, Zhang N, Wang R, Gao Y, Ran X, Sun Z, Zhang H, Yang G, Song X, Xu L. Performance of artificial intelligence in detecting the chronic total occlusive lesions of coronary artery based on coronary computed tomographic angiography. Cardiovasc Diagn Ther 2024. doi: 10.21037/cdt-23-407

Appendix 1

The explanation about the allocation of the training set and the testing set and determination of the sample size

This study was a diagnostic test, and the sample size was calculated using the area under the receiver operating characteristic (ROC) curve. The smallest area under the ROC curve was set as 0.90 according to the purpose of the study. Then, the type I error α was set as 0.05, and the type II error β was set as 0.1. The ratio of positive [chronic total occlusion (CTO) lesions] to negative (non-CTO lesions) was approximately 1:3. The results of MedCalc (version 18.11.3, MedCalc Software bvba, Ostend, Belgium) showed that the sample size required for clinical test was 19 patients, including 5 patients with CTO lesions and 14 patients with non-CTO lesions.

In order to ensure the robustness of the diagnostic model, we need to increase the amount of data in the training set as much as possible. So we randomly assigned the patients to the training dataset and the testing dataset at a rate of 4:1. According to the proportion of 4:1 (training set:testing set), the minimum required sample size of the training set was 76 patients, of whom 19 with CTO lesions and 57 with non-CTO lesions.

The artificial intelligence (AI) model requires a higher sample size than the conventional prediction model, and it is difficult to develop a robust model with only 95 patients. Therefore, to improve the robustness of our AI model, a total of 537 patients with 1,569 ICA-confirmed atherosclerotic lesions (including 672 lesions with <50% stenosis, 493 lesions with 50–99% stenosis, and 404 CTO lesions) were enrolled in this study.

Appendix 2

Convolutional neural network (CNN) was used to achieve myocardial and coronary artery segmentation and target lesion identification, which are feed-forward neuronal networks, and contain neurons with learnable weights and biases (24).The proposed deep learning framework, which consists of three models: (I) a two-stage 3D U-Net-based myocardium segmentation network to determine the coordinates of the heart contour and segment the myocardium fine structure; (II) a modified 3D U-Net for coronary segmentation, which includes encoding and decoding parts, and a connected growth prediction model (CGPM) to eliminate vascular segmentation errors and then avoid partial or missing vascular segments of CTO lesions effectively; and (III) a vessel-connect algorithm to identify the missing segments of the vessels and connect them with main branches, which in turn localizes and displays the region of CTO lesions (see main text *Figure 2*).

Detailed steps regarding our AI model development are shown as follows: for myocardial segmentation, an automatic segmentation framework was developed, which mainly consisted of two 3D U-Net networks, as shown in *Figure 2B*. The first 3D U-Net is used to determine the coordinates of the heart contour, while the other is used for the segmentation of the myocardium fine structure. For coronary segmentation, a modified 3D U-Net was used, which includes encoding and decoding parts, as shown in *Figure 2C*. The encoding part included four layers of down-sampling, and the decoding part included four layers of the up-sampling. Next, we added the bottleneck connection between down-sampling and up-sampling layers to maintain the multi-scale information in down-sampling process (30). After the 3D U-Net, a CGPM was used to eliminate vascular segmentation errors and then avoid partial or missing vascular segments effectively.

Due to the reduction in the contrast medium at the occlusion site or the distal vessel is prone to cause vessel segmentation errors, following which, the vessel segments were disconnected, and those before and after occlusion were difficult to be demonstrated in curved planar reconstruction (CPR) images. Therefore, we developed a new algorithm, combined with the imaging characteristics, to modify the extraction of the centerline and improve the detection of CTO lesions, as shown in *Figure 2D*.

The model utilized a novel algorithm, which enables automated extraction of the centerlines, to locate the CTO lesions by completing the missing segments. Based on previous myocardial segmentation and coronary segmentation results, the anatomical correlation between the centerline and myocardium location to distinct vessel branches was utilized. Subsequently, each branch of the centerline was labeled, and missing segments of the vessels were identified and connected with main branches, which in turn displayed and detected the CTO lesions. Details are as follows:

(I) On the coronary segmentation, the domain connected to the aorta was selected, the two largest connected domains on the coronary segmentation corresponding to the left and right branches of the coronary artery were identified, and the centerline of the vascular tree was extracted (31,32). The minimum distance between the nearest point

https://dx.doi.org/10.21037/cdt-23-407

of the left and right branches to the aorta and myocardium (left atrium, left ventricle, right atrium, and right ventricle) was termed as right coronary artery (RCA) and left main coronary artery (LM), respectively. According to the minimum distance between the bifurcation on the centerline of LM and myocardium and distinct left anterior descending artery (LAD) and left circumflex artery (LCX), the partial points on the centerline corresponding to the three main vessels were determined.

(II) The centerline was also extracted for the free connected domain that was not connected to the aorta in the coronary segmentation results. According to the positional correlation between the points on the centerline and the myocardium (left atrium, left ventricle, right atrium, and right ventricle), it was determined whether the free connected domain was the main vessel or its branch [posterior descending artery (PDA), diagonal branch (D), obtuse marginal (OM), ramus intermedius (RI), right posterior lateral branch (R-PLB)].

(III) If the centerline of connecting domain in step 2 was the main vessel, then based on the centerline in step 1, the nearest two points on the centerline of the free connected domain and the corresponding major branch in (II) are selected as the starting point and the ending point, respectively. Then, the path connecting the free connected domains to the three main vessels were computed by the minimum path algorithm.

(IV) According to the waypoint and centerline in step 3, the missing segments in the occlusion site lost in previous coronary segmentation results was complemented.

(V) Based on the results of the complemented coronary artery, the centerlines of the main vessels and their branches could be extracted such that the missing segments caused by CTO could also be detected on the straightened multiplanar reconstruction (MPR) and CPR.

References

30. Ronneberger O, Fischer P, Brox T. U-net: Convolutional networks for biomedical image segmentation. In: Navab N, Hornegger J, Wells W, et al. editors. Medical Image Computing and Computer-Assisted Intervention. Springer, Cham; 2015:234-41.
31. Oliveira DA, Leal-Taixé L, Feitosa RQ, et al. Automatic tracking of vessel-like structures from a single starting point. Comput Med Imaging Graph 2016;47:1-15.
32. Yang G, Kitslaar P, Frenay M, et al. Automatic centerline extraction of coronary arteries in coronary computed tomographic angiography. Int J Cardiovasc Imaging 2012;28:921-33.

https://dx.doi.org/10.21037/cdt-23-407